The Performance of Random Template Banks

Bruce Allen*
Max Planck Institute for Gravitational Physics (Albert Einstein Institute), Leibniz Universität Hannover, Callinstrasse 38, D-30167, Hannover, Germany
(Dated: March 10, 2022)

When searching for new gravitational-wave or electromagnetic sources, the n signal parameters (masses, sky location, frequencies,...) are unknown. In practice, one hunts for signals at a discrete set of points in parameter space, called a template bank. These may be constructed systematically as a lattice, or alternatively, by placing templates at randomly selected points in parameter space. Here, we calculate the fraction of signals lost by an n-dimensional random template bank (compared to a very finely spaced bank). This fraction is compared to the corresponding loss fraction for the best possible lattice-based template banks containing the same number of grid points. For dimensions $n < 4$ the lattice-based template banks significantly outperform the random ones. However, remarkably, for dimensions $n > 8$, the difference is negligible. In high dimensions, random template banks outperform the best known lattices.

I. INTRODUCTION

Many searches for gravitational-wave and electromagnetic signals are carried out using matched filtering, which compares instrumental data to waveform templates [1–3]. Because the parameters of the sources are not known a priori, many templates are required, forming a grid in parameter space [4–9]. Like the mesh on a fishing net, the grid needs to be spaced finely enough that signals don't slip through. But if the grid has far more points than are needed, the computational cost becomes excessive. For this reason, a substantial technology has evolved to create these grids [10–16] What choice of template bank is best?

The traditional literature on the topic asserts that, for a fixed number of grid points, the optimal template bank is the one that minimizes the maximum distance (twice the covering radius) between any grid point and its closest neighbor [10, 12, 13, 15, 17–20]. However, as recently shown in [21], this is incorrect.

If the goal is to maximize the number of detections and the templates are closely spaced, then the optimal template bank minimizes the *average mismatch*: the average squared distance between any point in parameter space and the closest grid point. The bank which minimizes this quantity (at fixed grid point density) is called the optimal quantizer. An extensive introduction to the topic of optimal quantizer lattices can be found in the remarkable book by Conway and Sloane [22], and an update on the current status in [23].

Lattice-based template banks can be challenging to construct. An alternative approach is to build template banks by placing search grid points *at random* [13] in parameter space. Because they are simple and quick to construct, and because they can easily accommodate arbitrary parameter-space constraints and boundaries, such "random template banks" are appealing [14, 24]. Note that random template banks may be improved by pruning away[25] grid points that are not needed. The result is then called a "stochastic template bank" [12].

Here, we provide a simple exact analysis of the performance of a random template bank. This could have been done a decade ago, when such template banks were introduced [13]. However, the authors of [13] (following the mistaken conventional wisdom described above, see [21, Section IV]) assessed the performance in terms of the covering radius [13] rather than in terms of the average mismatch.

Our analysis of random template bank performance has important consequences. We find that in low dimensions, a random template bank performs poorly in comparison with a well-chosen lattice. But as the dimension increases, the performance of a random template bank quickly approaches, and then surpasses the performance of even the best lattices.

This paper assumes that the reader is familiarity with [21], and is structured as follows. Section II defines the average mismatch $\langle r^2 \rangle$ in the usual quadratic approximation, and reviews its relationship to the fraction of signals lost and to the scale invariant second moment G of a lattice. Section III defines a random template bank as Poisson process in n dimensions, and calculates $\langle r^2 \rangle$ following an argument from [26]. This is compared to the best currently know lattices, and the best theoretically possible lattices. In Section IV we use results from [23] to calculate lost signals in template banks which are Cartesian products, since these are often used. In Section V we extend the results to cover the case of large mismatch, by replacing the normal quadratic approximation to the mismatch with the recently proposed spherical ansatz [27]. This is followed by a short conclusion.

The reader who is primarily interested in the results and not in the details should see Eq. (2.6) for the fraction f of lost detections, and then consult Fig. 1 and Table I. These show the performance of a random template bank, also comparing it to the best currently known lattice-based template banks, and to the best theoretically achievable template banks.

* bruce.allen@aei.mpg.de

II. AVERAGE MISMATCH AND THE SECOND MOMENT G

As we have explained, the performance of a template bank is determined by the average mismatch [21]. For a given region of parameter space and a given number of grid points, this in turn is proportional to the scale invariant second moment G.

To define G and show it's relationship to the average mismatch, let $x \in \mathbb{R}^n$ be parameter-space coordinates, and let $\mathcal{V} \subset \mathbb{R}^n$ be the region of interest (for example corresponding to the desired ranges of masses and frequencies of interest in a search). Here, x denotes a vector with n Cartesian components, and we employ the standard Euclidean metric and norm.

The parameter-space n-volume is $V = V(\mathcal{V})$, where

$$V(\mathcal{S}) = \int_{\mathcal{S}} d^n x, \tag{2.1}$$

is the volume of some subset $\mathcal{S} \subset \mathbb{R}^n$.

Suppose that N search templates are located at grid points $x_1, \dots, x_N$. Define the mismatch function

$$r^2(x) = \min(|x - x_1|^2, |x - x_2|^2, \dots, |x - x_N|^2), \tag{2.2}$$

which is the squared distance from x to the nearest template. For the given template bank it is the fractional loss in (squared) signal-to-noise ratio (SNR) at each point in parameter space. The average of this quantity,

$$\langle r^2 \rangle = \frac{1}{V} \int_{\mathcal{V}} r^2(x) d^n x, \tag{2.3}$$

is the *average mismatch* [28]

The goal of the template-bank architect is to minimize the average mismatch. This is because the fraction of signals which are lost (compared to a template bank with a very finely spaced grid) is given by [21, Eq. (5.6)]

$$f = \frac{D}{2} \langle r^2 \rangle, \tag{2.4}$$

where D is the effective dimension of the source distribution, which usually lies in the range $2 < D < 3$. (See [21, Eq. (5.1)] for the definition of the source distribution function, and note that here, to avoid confusion with the differential symbol, we use D rather than d to denote the dimension of the source distribution.)

For example, suppose that 100 sources would in principle be detectable with a very finely spaced template bank, and that these sources were distributed uniformly in space ($D = 3$). Then a template bank with an $\langle r^2 \rangle = 3\%$ average mismatch loses about $f = 5\%$ of potential detections, so on average 95 sources would be detected and 5 would be lost.

To compare the relative performance of different template banks (i.e., different choices of the N grid point locations x_i), it is convenient to define the *scale-invariant second moment*

$$G = \frac{1}{n} \frac{\langle r^2 \rangle}{(V/N)^{2/n}}. \tag{2.5}$$

Note that our definition in Eq. (2.5) is the conventional one [22, Ch 2 Eq (87)], in spite of the appearance of N. This is because in the conventional definition, V denotes the volume per grid point, which here is V/N.

The performance indicator f, which is the fraction of potentially detectable signals that are lost because of the discreteness of the template bank, may be expressed in terms of G, as

$$f = \tfrac{1}{2} n \, D (V/N)^{2/n} G. \tag{2.6}$$

Here, the "effective source dimension" D is set by the spatial distribution of signal sources, and V/N is the parameter-space volume per grid point.

To compare the performance of different template banks, fix the number of templates N, the parameter space dimension n, and the volume of parameter space V. Then, the template grid with the smallest G is the best choice, since it loses the smallest fraction of detections.

The simplest lattice, which is the n-dimensional cubic lattice, has a dimensionless second moment $G(\mathbb{Z}^n) = 1/12 \approx 0.08333$. A table showing the current records for the smallest G among lattices (and also comparing the covering thickness) can be found in [21] and a larger and more recent table in [23]; these latter values are also shown in Fig. 1.

III. RANDOM TEMPLATE BANKS

We now compute the performance of a random template bank. As first proposed by [13], this is created by randomly placing grid points uniformly within $\mathcal{V}$, locating each point independently of the positions of the other points. Here, "uniformly" means a Poisson process: the probability of finding a grid point within an infinitesimal volume dV is

$$P = \rho \, dV, \tag{3.1}$$

where $\rho = N/V$ is the density of grid points: the number of grid points per unit parameter-space volume.

By standard arguments for Poisson processes [30, Chapter 14-4], the probability of finding ℓ points within a finite volume v is

$$P(\ell) = \frac{(\rho v)^\ell}{\ell!} \mathrm{e}^{-\rho v}. \tag{3.2}$$

Here, and throughout, we assume that N is large enough that truncating this distribution for $\ell > N$ has no significant effect, or equivalently, that the n-volume $V \to \infty$ with the density of grid points ρ held constant, or equivalently, that the volume v under consideration is small compared to V, so that $v/V << 1$.

We now calculate $\langle r^2 \rangle$ and G following a beautiful argument [31] given by Torquato in [26]. Let $E(r)$ denote the *empty probability*. This is the probability that an

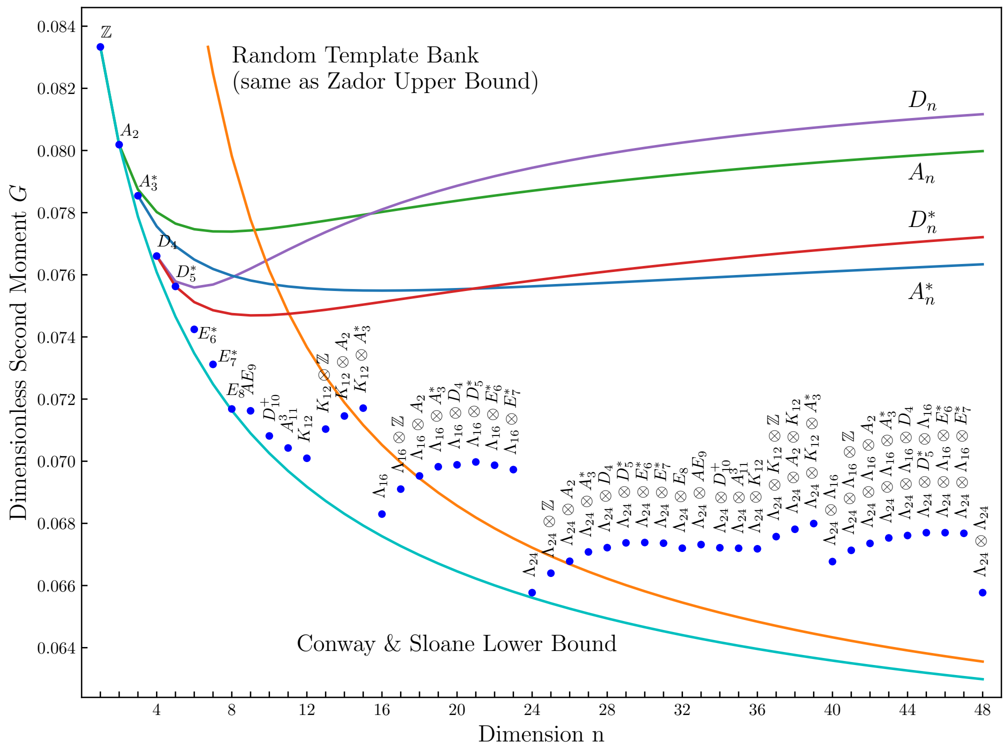

FIG. 1. The current record-holding (smallest G) lattice template banks [23, Table 1] (blue points) lie above the conjectured Conway & Sloane [29] lower bound (cyan curve). The random template bank G (orange) has its performance given by the Zador upper bound Eq. (3.8). For a fixed number of grid points, in dimensions $n > 8$, a random template bank has a performance (detection loss) which is within 10% of the theoretically best possible template bank (see Table I). In many higher dimensions (for example 15 or 19) the random template bank outperforms *any* known lattice.

n-ball of radius r, randomly placed in parameter space, contains no grid points. The ball's n-volume is

$$V(B(r)) = \frac{\pi^{n/2}}{\Gamma(1+n/2)}\, r^n, \tag{3.3}$$

where the gamma function is defined by

$$\Gamma(z) = \int_0^\infty t^{z-1} \mathrm{e}^{-t} dt \tag{3.4}$$

on the half-plane $\Re(z) > 0$, and by analytic continuation elsewhere. Setting $\ell = 0$ in Eq. (3.2), the empty probability is

$$E(r) = P(0) = \mathrm{e}^{-\rho V(B(r))}. \tag{3.5}$$

Now, by definition, $E(r+dr)$ is the probability that a slightly larger ball of radius $r + dr$, randomly placed in parameter space, contains no grid points. This is a bit smaller than $E(r)$, and the difference,

$$E(r) - E(r+dr) = -\frac{dE}{dr}\, dr, \tag{3.6}$$

is the probability that the closest grid point to a random point x lies in the shell of radius $r \in (r, r+dr)$ from x.

Since $-\frac{dE}{dr}\, dr$ is the probability that the closest grid point lies in the shell of radius $(r, r+dr)$, it follows immediately that the average squared distance to the closest point in the template bank is

$$\begin{aligned} \langle r^2 \rangle &= -\int_0^\infty r^2 \frac{dE}{dr} dr \\ &= 2\int_0^\infty r E(r) dr \\ &= \frac{1}{\pi} \rho^{-\frac{2}{n}} \Gamma(1+\tfrac{n}{2})^{\frac{2}{n}} \Gamma(1+\tfrac{2}{n}), \end{aligned} \tag{3.7}$$

where on the second line we have integrated by parts, and on the third line we have substituted Eq. (3.5), changed variables, and used the definition Eq. (3.4) of the gamma function, along with $z\Gamma(z) = \Gamma(z+1)$.

The scale-invariant second moment G of the random template bank follows from Eqs. (2.5) and (3.7), since $\rho = N/V$. This reproduces [26, Eq. (99)], and furthermore, as noted by Torquato, gives exactly the Zador upper bound [32] for the optimal scale-invariant second moment

$$\begin{aligned} G_{\text{Random}} &= G_{\text{Zador upper}} \\ &= \frac{1}{n\pi} \Gamma(1+\tfrac{n}{2})^{\frac{2}{n}} \Gamma(1+\tfrac{2}{n}). \end{aligned} \tag{3.8}$$

This is plotted as the orange curve in Fig. 1.

n	$G_{\rm CS}$	$G_{\rm random}$	Max Gain %
1	0.08333	0.50000	500
2	0.08019	0.15915	98.5
3	0.07787	0.11580	48.7
4	0.07609	0.09974	31.1
5	0.07465	0.09132	22.3
6	0.07347	0.08608	17.2
7	0.07248	0.08248	13.8
8	0.07163	0.07982	11.4
9	0.07090	0.07778	9.7
10	0.07026	0.07614	8.4
11	0.06969	0.07480	7.3
12	0.06918	0.07367	6.5
13	0.06872	0.07272	5.8
14	0.06831	0.07189	5.2
15	0.06793	0.07116	4.8
16	0.06759	0.07053	4.3

TABLE I. An ideal template bank has a loss factor G at the Conway & Sloane lower bound $G_{\rm CS}$, whereas a random template bank has a loss factor of $G_{\rm random}$. The final column shows the fractional difference in percent. For example, in $n = 9$ dimensions, if an ideal template bank were spaced to lose 5% of detectable signals, then s random template bank with the same number of grid points would lose about 5.5% of detectable signals (9.7% more).

As can be seen from Fig. 1 and Table I, the performance of a random template bank is very dependent upon dimension. In small dimensions, the performance is poor. For example in one dimension, for a given parameter space volume, signal source, and number of templates, a one-dimensional random template bank loses six times as many signals as the uniformly spaced grid $\mathbb{Z}$. In dimension two, the random template bank loses almost twice as many signals as the hexagonal lattice A_2, and in dimension three, it loses about 47% more signals than the optimal quantizer, which is the body-centered-cubic (bcc, A_3^*) lattice. But the relative performance of a random template bank improves rapidly with dimension. By dimension 7, its performance is better than that of the hyper-cubic lattice $\mathbb{Z}^n$. By dimension 8, the random template bank loses only 11% more signals than the best known quantizer lattice E_8, which is likely optimal [33].

As the parameter space dimension $n \to \infty$, both the Conway & Sloane conjectured lower bound and the Zador upper bound approach $G_\infty = 1/2\pi e \approx 0.058549$. In this sense, in higher dimensions, a random template bank, whose performance is equal to the Zador upper bound, is as good as one can get. In practice, this limit is quickly reached. If one selects a random template bank, then the final column of Table I shows the maximum fractional improvement (decrease from optimal) that is possible if there were a lattice that lies on the Conway & Sloane conjectured lower bound. This potential fractional improvement drops below 10% in dimension 8, and below 5% in dimension 15.

IV. PRODUCT TEMPLATE BANKS

It is often desirable to construct a template bank as the Cartesian product of two lower-dimensional template banks. For example, if one of the parameter space dimensions is frequency, and the signal-to-noise statistics are obtained via a fast Fourier transform (FFT) from time-domain data. Such an FFT yields evenly-spaced frequency bins. As a second example, if one of the parameter space dimensions is binary coalescence time, and it is sampled at the same sample rate as the data, or at some sub-harmonic of that rate. In both examples, the parameter space grid then has a factor which is the evenly-spaced one dimensional lattice $\mathbb{Z}$.

In the most general approach to such cases, the template bank on the full n-dimensional parameter space is the Cartesian product of two lower-dimensional template bank "factors", whose dimensions are n_a and n_b, with $n = n_a + n_b$. Recent work [23] shows how the relative grid-spacings of the two factors can be scaled or adjusted to achieve the smallest possible value of G for the resulting product. After that scaling, the product template bank has a scale-invariant second moment given by [23, Eq. (41)]

$$G = G_a^{\frac{n_a}{n}} G_b^{\frac{n_b}{n}}, \tag{4.1}$$

where G_a and G_b are the scale-invariant second moments of the two factors. Since $G(\mathbb{Z}) = 1/12$, the one dimensional examples above correspond to $n_a = 1$ and $G_a = 1/12$.

In this way, the results of this paper can also be used to characterize the optimal performance of template banks that are constructed as a product of a random template bank with a lattice, or of two independent random template banks.

V. LOSS FRACTION AT LARGE MISMATCH

Up to this point in the paper, we have only considered "closely spaced" random template banks. We now generalize those results to arbitrarily large spacing. To distinguish these two cases, it is helpful to define

$$\Delta = \rho^{-1/n} = \left(\frac{V}{N}\right)^{1/n}, \tag{5.1}$$

which is the *characteristic distance* between grid points.

If the templates are closely spaced, then Δ is small. From Eqs. (2.4) and (3.7), this ensures that the fraction of lost signals

$$f = \frac{D}{2\pi}\Gamma(1+\tfrac{n}{2})^{\frac{2}{n}}\Gamma(1+\tfrac{2}{n})\,\Delta^2 \tag{5.2}$$

is small: $f << 1$. However, the treatment in Section III clearly breaks down if the grid spacing Δ becomes too large, since in that case the loss fraction f in Eq. (5.2) would exceed unity. This is inconsistent, since by definition $f \le 1$. This inconsistency arises because Section III assumes the "quadratic approximation" to the mismatch, which is is invalid for large separations.

In this Section, we make use of the "spherical ansatz" of [27] to compute the loss fraction of a random template bank for arbitrarily large template grid spacing Δ. As before, the calculation for a random template bank is much simpler than for a lattice.

Employing the spherical ansatz, the loss fraction of Eq. (2.4) $f = D\langle r^2\rangle/2$ is replaced by

$$f = \langle s(r)\rangle, \tag{5.3}$$

where

$$s(r) = \begin{cases} 1 - \cos^D r & \text{for } r \le \pi/2, \text{ and} \\ 1 & \text{for } r > \pi/2. \end{cases} \tag{5.4}$$

(These equations are derived in [27, Eq. (5.10)] and [34, Eqns. (3.6) and (3.7)]. When r is small, expansion of Eq. (5.4) in a Taylor series for small r gives $s(r) \approx Dr^2/2$, recovering Eq. (2.4).)

To calculate $\langle s(r)\rangle$ we proceed as in Section III) beginning with Eq. (3.7) to obtain

$$\begin{aligned} \langle s(r)\rangle &= -\int_0^\infty s(r)\frac{dE}{dr}dr \\ &= \int_0^\infty \frac{ds(r)}{dr}E(r)\,dr \\ &= \int_0^{\pi/2} E(r)\frac{d}{dr}(1-\cos^D r)\,dr. \end{aligned} \tag{5.5}$$

In the second line we have integrated by parts, since $s(r)$ vanishes at $r = 0$ and $E(r)$ vanishes as $r \to \infty$. The third line follows because the derivative of $s(r)$ vanishes for $r > \pi/2$.

To compute this in closed form, we rewrite the integral in terms of the "expected values" of even powers of r. (These are defined as in [21, Eq. (5.11)], with the caveat that the corresponding integrals are truncated at $r = \pi/2$. To emphasize this, we use R rather than r inside the angle brackets.) Thus we define the *truncated moments*

$$\begin{aligned} \langle R^p\rangle &= \int_0^{\pi/2} E(r)\,\frac{d}{dr}r^p\,dr \\ &= \frac{p}{n}\Delta^p\pi^{-\frac{p}{2}}\,\Gamma(1+\frac{n}{2})^{\frac{p}{n}}\,\gamma\Big(\frac{p}{n}, \frac{\pi^{\frac{3}{2}n}}{2^n\Delta^n\Gamma(1+\frac{n}{2})}\Big), \end{aligned} \tag{5.6}$$

where the *lower incomplete gamma function* is defined by

$$\gamma(z,x) = \int_0^x t^{z-1}\mathrm{e}^{-t}dt. \tag{5.7}$$

To use these moments to compute the loss fraction from Eq. (5.5), first expand $\cos^D r$ in a Taylor series, and then replace the (even) powers of r using Eq. (5.6). One obtains the loss fraction $f = \langle s(r)\rangle$ given by

$$\begin{aligned} f = \frac{D}{2}\langle R^2\rangle - \frac{3D^2-2D}{24}\langle R^4\rangle + \frac{15D^3-30D^2+16D}{720}\langle R^6\rangle \\ - \frac{105D^4-420D^3+588D^2-272D}{40320}\langle R^8\rangle + \ldots. \end{aligned}$$

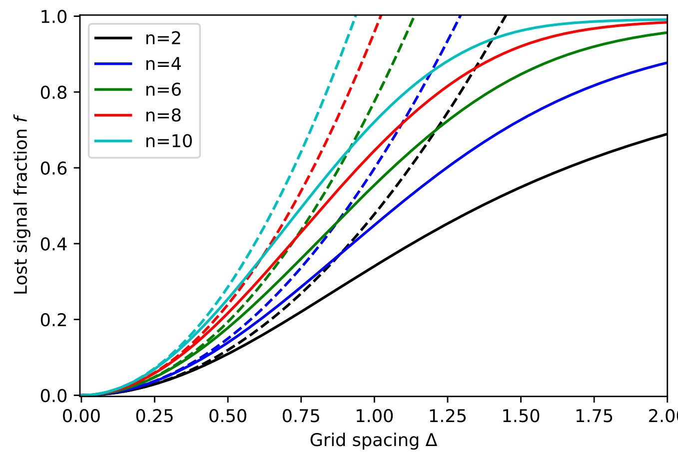

FIG. 2. The fraction of signals which are lost by a random template bank as function of the grid spacing Δ. These are computed using the spherical ansatz for the mismatch, for a D=3–dimensional source distribution; the curves show parameter-space dimensions $n = 2, 4, \ldots, 12$. The dashed lines show the quadratic approximation for the mismatch, which is accurate at small grid spacings.

The loss fractions f for random template banks are shown in Figure 2 for a $D = 3-$dimensional source distribution. Note that while Eq. (5.8) does not show the expansion terms proportional to $\langle R^{10}\rangle$ and $\langle R^{12}\rangle$, these are nevertheless included in Figure 2, providing accuracy substantially greater than the plotting line width.

VI. CONCLUSION

Random template banks are practical to employ because they are quick and simple to construct. It is remarkable that their performance is so easily characterized.

This analysis would have been possible when random template banks were first introduced [13]. However, as we have explained, the authors of that work were focused on the covering radius, or more strictly speaking, on the "effective covering radius". Here, "effective" means that a specified (large) fraction of the parameter space was within a region covered by balls of the specified radius. This approach was necessary, because the covering radius is defined by the first positive root of the empty probability $E(r)$. But, as can be seen from Eq. (3.5), in the case of a random template bank, $E(r)$ has no positive roots. Hence the authors of [13] made use of an effective covering radius, at which $E(r)$ had decreased to an acceptably small value. This leads to a more complex treatment than the one given here.

For simplicity in this short paper, we have concentrated on the simplest case, with a flat parameter-space metric. However, these results also apply to the non-flat case, provided that the density of grid points is large enough to ensure that the signal manifold around each grid point is well approximated by flat space in the vicinity of the nearest neighboring n grid points. If so, then a Poisson random template bank may be created by placing grid points with a constant probability density per unit volume $dV = \sqrt{\det g_{ab}}\, d^n x$, where g_{ab} is the parameter space metric. This could also be modified to account for a varying probability of sources, as in [21, Section VI].

These results should be of use in constructing and characterizing template banks, and in understanding to what degree those template banks might be improved.

VII. ACKNOWLEDGMENTS

I acknowledge Erik Agrell, Daniel Pook-Kolb, and Andrey Shoom for many interesting discussions about lattices, Chris Messenger, Ben Owen, Maria Alessandra Papa, Reinhard Prix, and B.S. Sathyaprakash for many interesting discussions about template banks, and Salvatore Torquato for helpful correspondence.

[1] B. F. Schutz, REVIEW ARTICLE: Gravitational wave sources and their detectability, Classical and Quantum Gravity **6**, 1761 (1989).

[2] B. F. Schutz, Data Processing Analysis and Storage for Interferometric Antennas, in *The Detection of Gravitational Waves*, edited by D. G. Blair (1991) p. 406.

[3] B. Allen, W. G. Anderson, P. R. Brady, D. A. Brown, and J. D. E. Creighton, Findchirp: An algorithm for detection of gravitational waves from inspiraling compact binaries, Phys. Rev. D **85**, 122006 (2012).

[4] B. S. Sathyaprakash and S. V. Dhurandhar, Choice of filters for the detection of gravitational waves from coalescing binaries, Phys. Rev. D **44**, 3819 (1991).

[5] L. S. Finn and D. F. Chernoff, Observing binary inspiral in gravitational radiation: One interferometer, Phys. Rev. D **47**, 2198 (1993).

[6] S. V. Dhurandhar and B. S. Sathyaprakash, Choice of filters for the detection of gravitational waves from coalescing binaries. II. Detection in colored noise, Phys. Rev. D **49**, 1707 (1994).

[7] C. Cutler and É. E. Flanagan, Gravitational waves from merging compact binaries: How accurately can one extract the binary's parameters from the inspiral waveform?, Phys. Rev. D **49**, 2658 (1994).

[8] B. S. Sathyaprakash, Filtering post-Newtonian gravitational waves from coalescing binaries, Phys. Rev. D **50**, R7111 (1994).

[9] B. J. Owen, Search templates for gravitational waves from inspiraling binaries: Choice of template spacing, Phys. Rev. D **53**, 6749 (1996).

[10] R. Prix, Template-based searches for gravitational waves: efficient lattice covering of flat parameter spaces, Classical and Quantum Gravity **24**, S481 (2007).

[11] S. Babak, Building a stochastic template bank for detecting massive black hole binaries, Classical and Quantum Gravity **25**, 195011 (2008).

[12] I. W. Harry, B. Allen, and B. S. Sathyaprakash, Stochastic template placement algorithm for gravitational wave data analysis, Phys. Rev. D **80**, 104014 (2009).

[13] C. Messenger, R. Prix, and M. A. Papa, Random template banks and relaxed lattice coverings, Phys. Rev. D **79**, 104017 (2009).

[14] G. M. Manca and M. Vallisneri, Cover art: Issues in the metric-guided and metric-less placement of random and stochastic template banks, Phys. Rev. D **81**, 024004 (2010).

[15] H. Fehrmann and H. J. Pletsch, Efficient generation and optimization of stochastic template banks by a neighboring cell algorithm, Phys. Rev. D **90**, 124049 (2014).

[16] S. Roy, A. Sankar Sengupta, and P. Ajith, Geometric-stochastic template banks for gravitational wave searches from compact binaries in advanced-LIGO data, in *42nd COSPAR Scientific Assembly*, Vol. 42 (2018) pp. E1.15–36–18.

[17] C. Van Den Broeck, D. A. Brown, T. Cokelaer, I. Harry, G. Jones, B. S. Sathyaprakash, H. Tagoshi, and H. Takahashi, Template banks to search for compact binaries with spinning components in gravitational wave data, Phys. Rev. D **80**, 024009 (2009).

[18] P. Jaranowski and A. Krolak, *Analysis of Gravitational-Wave Data* (Cambridge University Press, 2009).

[19] N. Indik, K. Haris, T. Dal Canton, H. Fehrmann, B. Krishnan, A. Lundgren, A. B. Nielsen, and A. Pai, Stochastic template bank for gravitational wave searches for precessing neutron-star-black-hole coalescence events, Phys. Rev. D **95**, 064056 (2017).

[20] T. Dal Canton and I. W. Harry, Designing a template bank to observe compact binary coalescences in Advanced LIGO's second observing run, arXiv e-prints , arXiv:1705.01845 (2017).

[21] B. Allen, Optimal template banks, Phys. Rev. D **104**, 042005 (2021).

[22] J. H. Conway and N. J. A. Sloane, *Sphere packings, lattices and groups, third Edition*, Vol. 290 (Springer Science & Business Media, 1999).

[23] E. Agrell and B. Allen, On the best lattice quantizers (2022), arXiv:2202.09605 [cs.IT].

[24] S. Roy, A. S. Sengupta, and N. Thakor, Hybrid geometric-random template-placement algorithm for gravitational wave searches from compact binary coalescences, Phys. Rev. D **95**, 104045 (2017).

[25] To date, the pruning algorithms are tuned to increase the covering radius rather than to decrease the dimensionless second moment. In light of [21] there is also room for improvement here.

[26] S. Torquato, Reformulation of the covering and quantizer problems as ground states of interacting particles, Phys. Rev. E **82**, 056109 (2010).

[27] B. Allen, Spherical ansatz for parameter-space metrics, Phys. Rev. D **100**, 124004 (2019).

[28] See [21, Section II after Eq. (2.5)] for a discussion of the different ways in which the term "mismatch" is used in the literature.

[29] J. Conway and N. Sloane, A lower bound on the average error of vector quantizers (corresp.), IEEE Transactions on Information Theory **31**, 106 (1985).

[30] J. Mathews and R. L. Walker, *Mathematical Methods of Physics*, 2nd ed. (Addison-Wesley, New York, 1970).

[31] In [26], Eq. (48) should read "Probability that the *closest* point of the point process..."; this is correct in [35, Eq. (2.88)]. In [26], the sentence before Eq. (99) should read "Substitution of Eq. (60) into Eq. (75) and use of Eq. (96) at unit density yields...".

[32] P. L. Zador, Asymptotic quantization error of continuous signals and the quantization dimension, IEEE Trans. Inf. Theory **IT-82**, 139 (1982).

[33] There are no rigorous proofs of optimality for quantizers in dimensions $n > 3$ [23]. However there is a remarkable proof that E_8 is the optimal solution for the 8-dimensional sphere packing problem [36, 37] and we consider it very likely that E_8 is also the optimal quantizer in 8 dimensions.

[34] B. Allen and A. A. Shoom, Template banks based on Z^n and A_n^* lattices, Phys. Rev. D **104**, 122007 (2021).

[35] S. Torquato, *Random Heterogeneous Materials: Microstructure and Macroscopic Properties*, Interdisciplinary Applied Mathematics, Vol 16 (Springer, 2002).

[36] M. Viazovska, The sphere packing problem in dimension 8, Annals of Mathematics **185**, 991 (2017).

[37] H. Cohn, A conceptual breakthrough in sphere packing, Notices Amer. Math. Soc. **64**, 102 (2017).